Spontaneous Symmetry Breaking of Population in a Nonadiabatically Driven Atomic Trap: An Ising-Class Phase Transition

Kihwan Kim,[1,2] Myoung-Sun Heo,[1,2] Ki-Hwan Lee,[1,2] Kiyoub Jang,[1,2] Heung-Ryoul Noh,[3] Doochul Kim,[1] and Wonho Jhe[1,2,*]

[1]*School of Physics, Seoul National University, Seoul 151-747, Korea*
[2]*Center for Near-Field Atom-Photon Technology, Seoul National University, Seoul 151-747, Korea*
[3]*Department of Physics, Chonnam National University, Gwangju 500-757, Korea*
(Received 5 July 2005; revised manuscript received 19 September 2005; published 19 April 2006)

We have observed spontaneous symmetry breaking of the population of Brownian particles between two *moving* potentials in the spatiotemporally symmetric system. Cold atoms preferentially occupy one of the dynamic double-well potentials, produced in the parametrically driven dissipative magneto-optical trap far from equilibrium, above a critical number of atoms. We find that the population asymmetry, which may be interpreted as the biased Brownian motion, can be qualitatively described by the mean-field Ising-class phase transition. This *in situ* study may be useful for investigation of dynamic phase transition or temporal behavior of critical phenomena.

DOI: 10.1103/PhysRevLett.96.150601 PACS numbers: 05.70.Fh, 05.45.−a, 32.80.Pj, 68.35.Rh

The Brownian motion of randomly fluctuating particles is, in general, isotropic in space, with no preferred direction of motion. However, the problem of directional Brownian motion due to nonequilibrium fluctuations has been extensively studied in diverse contexts from basic sciences to molecular engineering [1]. In most cases, the system of interest is anisotropic because the asymmetry in spatial inversion [2] or temporal translation [3] is externally imposed, which results in the biased diffusive motion of the Brownian particles, or the left-right symmetry breaking.

On the other hand, it has been known that, even in the system possessing the spatiotemporal symmetry, the left-right asymmetry of the Brownian motion may occur due to interparticle interactions, which leads to a possible realization of Maxwell's demon [4]. The unique experiment was the observation of spontaneous symmetry breaking (SSB) of the population of the vibration-fluidized granular particles between two symmetric, *stationary* compartments partitioned by a physical wall with a small hole, so that only one of the two compartments was preferentially occupied by the particles due to their inelastic collisions [5]. Since this is the only example, more experimental study is needed, in particular, because there is little known about such SSB transition in systems far from equilibrium.

In this Letter, we report on SSB of the population of the Brownian particles between two symmetric, *moving* compartments in the spatiotemporally symmetric system. We have used cold atoms in the parametrically driven magneto-optical trap (MOT), which is equivalent to a dynamic double-well potential system [6], or a system of two symmetrically oscillating electromagnetic "compartments" connected by an optical "hole." Laser-induced cooperative effects [7,8] on atomic transition between the two moving potentials are responsible for SSB, which plays the role of a narrow channel connecting them. In particular, it is interesting to find that the SSB of the left-right atomic population that occurs above a critical number of atoms can be qualitatively understood by the Ising-class phase transition associated with the spontaneous breaking of the $Z(2)$ symmetry [9].

Our experimental setup is the typical six-beam MOT where one pair of counterpropagating trapping lasers is intensity modulated, resulting in parametric resonance. In this system, we observed limit cycles (i.e., phase-space orbit attractors) and super- and subcritical Hopf bifurcation [6]. The limit cycle is manifested as two atomic states oscillating with opposite phases and finite amplitudes, when projected onto position space (Fig. 1). Moreover, the bifurcations were analyzed by atomic double- and

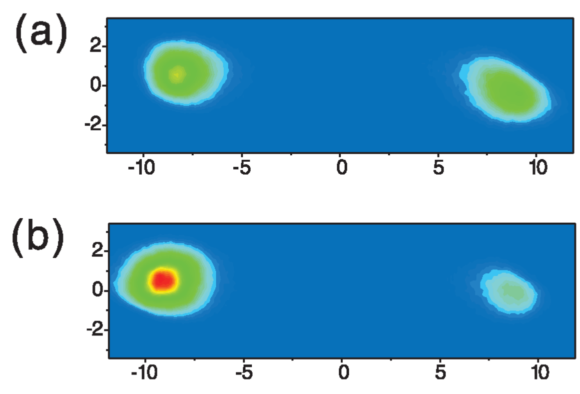

FIG. 1 (color). Typical snapshot images of atoms in two dynamic attractors (a) before SSB of atomic population and (b) after SSB, taken by a charge-coupled-device (CCD). The total number of atoms is (a) 6.1×10^7 and (b) 6.9×10^7, respectively, and the relative population difference in (b) is 0.63. Here the abscissas are in units of mm.

triple-well potentials available in the rotating phase space. In particular, due to fluctuating atomic motions resulting from spontaneous emissions, atomic population transfer occurs between the two states of dynamic double well, which tends to equalize each population [Fig. 1(a)] [10].

It is interesting to obtain such population symmetry, which is equivalent to zero spontaneous magnetization in the Ising spin system, only below a certain critical value of the total atomic number. Above the critical number, however, we observed SSB of atomic population, as shown in Fig. 1(b). The SSB was achieved under wide experimental conditions of modulation frequency f and amplitude h, from supercritical to subcritical bifurcation regions. The cooling laser intensity in the atomic oscillation direction (z axis) was $I_z = 0.039 I_s$ (I_s is the averaged saturation intensity, 3.78 $\mathrm{mW/cm^2}$), which was 5 times smaller than that of the transverse axes. The measured trap frequency along the z axis, f_0, was 43.6($\pm$2.4) Hz and the damping coefficient, γ, was 160.4($\pm$33) $\mathrm{s^{-1}}$.

Figure 2(a) presents the normalized population difference between the two dynamic states (1 and 2, with $N_1 > N_2$), $\Delta_p = (N_1 - N_2)/N_T$ versus the total atomic number, $N_T = N_1 + N_2$. As is shown, the main control parameter of SSB is N_T so that SSB occurs above the critical number N_c. We have measured N_1 and N_2 *in situ* by two independent methods: weak-probe absorption (empty boxes) and CCD images (filled black boxes, with error bars smaller than the data points). N_T was varied by adjusting the intensity of the repumping laser while all the other trap parameters remain fixed. Note that we did not find any control parameters other than N_T: for instance, the intensity imbalance between the $+z$ and $-z$ laser beams did not contribute to SSB for the imbalance of up to 20%, beyond which the atomic limit-cycle motions were not sustained.

For a detailed understanding of SSB, we have investigated the temporal evolution of the populations of each state when SSB occurs. Figure 2(b) shows the atomic populations recorded by probe absorption. As can be found, in the initial loading stage, the number of atoms in each state increases at the same rate and their growth is indistinguishable with each other. When the loading process is finished at about 20 s elapse, however, the population of one state increases whereas the other state is depopulated, as shown in the lower split curves. The fact that the total atomic number is conserved within experimental errors during the SSB process, shown in the upper curve, indicates that SSB originates not from different loading rates to each state but from the transfer of atoms between the two states. Moreover, when we place a kicking laser near the center of the two dynamic states in order to block any atomic transfer, the population symmetry is recovered. This evidence confirms that SSB occurs due to the anisotropic atomic transitions between the two states. Note that SSB process is always random and symmetric; there is an equal probability of having higher population in one of the two states when the experiments are repeated many times above the critical number.

For a systematic study of SSB, we have measured the critical number N_c from the data shown in Fig. 2(a) at various values of f and h. The results presented in Figs. 3(a) and 3(b) may be intuitively understood as follows. As f or h is increased, the maximum separation between the two oscillating states increases, which results in the decrease of the atomic transition rate W due to the increased distance between the two potential wells [10]. N_c will then decrease as W is decreased, because the smaller W makes it less likely to maintain the population symmetry. Note that SSB was not observed below the supercritical ($f = 1.93 f_0$) or above the subcritical bifurcation point ($f = 2.4 f_0$). This is expected because near the supercritical bifurcation point, W becomes too large to load atoms enough to produce SSB (i.e., N_c becomes too large). On the other hand, near the subcritical bifurcation point, only the population of the central stationary state among the triple wells increases despite the low N_c, whereas the two dynamic states are not populated above N_c, so that SSB does not occur.

Based on the fact that SSB appears above the critical number, one may conjecture that SSB is due to the collective effects of atoms occurring between the two dynamic states [11,12]. There are two such collective mechanisms for the MOT atoms. One is the shadow effect resulting from

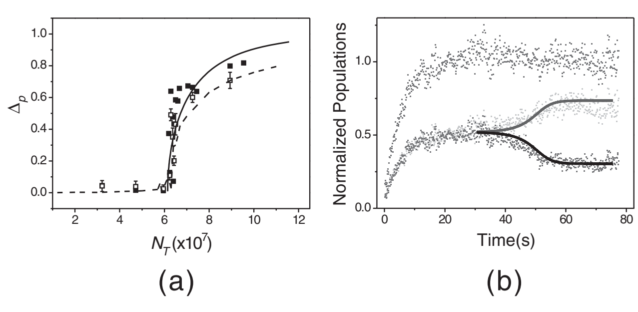

FIG. 2. (a) Measurement of Δ_p vs N_T. Here $f = 2.0 f_0$ and $h = 0.86$. The solid curve shows the Ising-model function, Eq. (4), with $N_c = 6.2(\pm 0.4) \times 10^7$. The dotted curve represents the Monte Carlo simulations performed with 10^3 atoms. (b) Temporal evolution of SSB. The solid curves represent the simulation results ($N_T = 6.5 \times 10^7$ and $\Delta_p = 0.52$).

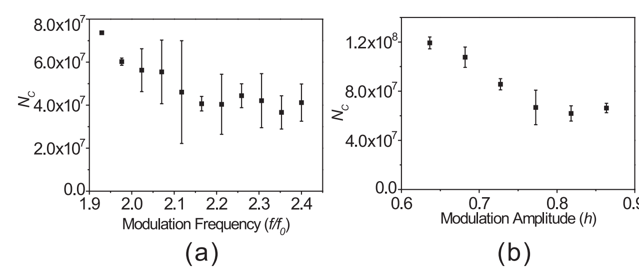

FIG. 3. N_c measured at various experimental parameters, (a) at fixed $h = 0.95$ and (b) at fixed $f = 2.1 f_0 (= 91$ Hz).

absorption of the cooling lasers by atoms in one state, causing the reduction of the laser intensity for atoms in the other state. The other is the reradiation effect that arises when an atom reabsorbs photons emitted by another atom, which produces the repulsive forces between them. The reradiation effect, in fact, contributes as an obstacle to SSB. As the number of atoms in one of the two states becomes dominated due to fluctuations, the repulsive reradiation force becomes bigger near the more-populated atomic cloud. Thus, this effect prevents atoms in the smaller-number state from being transferred to the larger-number state, which results in the recovery of population symmetry between the two states. On the other hand, the shadow effect further enhances the population asymmetry: the bigger shadow effect by the larger-number state pulls more atoms toward it.

For the theoretical description of SSB process, we adopt the phase-space Hamiltonian-function formalism [13] and generalize to include the shadow effect as well as the reradiation force. We start from the Doppler equation of the driven MOT in the z axis, expanded up to third order in z, which is written as

$$\ddot{z} + \gamma\dot{z} + (2\pi f_0)^2(1 + h\cos 2\pi f t)z + A_0(2\pi f_0)^2 z^3 = 0, \quad (1)$$

where A_0 is the coefficient of the third-order term, as introduced in [6]. From Eq. (1), one can easily derive the phase-space Hamiltonian function of an ith atom without the collective effects as

$$H_i^0(X_i, Y_i) = \tfrac{1}{2}(\mu - 1)X_i^2 + \tfrac{1}{2}(\mu + 1)Y_i^2 - \tfrac{1}{4}(X_i^2 + Y_i^2)^2, \quad (2)$$

which is plotted in Fig. 4(a) $[\mu = 2(f - 2f_0)/hf_0]$. Here X_i and Y_i are the two scaled canonical variables, associated with the coordinate and momentum variables, in the rotating phase space in which each state is instantaneously at rest. Note that the right(left)-side cloud with respect to the center of the limit-cycle motion in the z axis corresponds to the positive (negative) state in the Y axis at a given modulation phase of 0°.

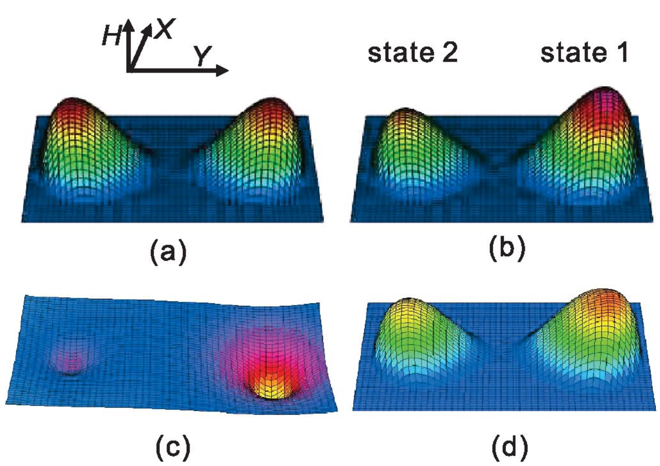

FIG. 4 (color). (a) $H_i^0(X_i, Y_i)$, showing the population symmetry. (b) $H_i^0 + H_i^S$ with the shadow effect included, which leads to SSB. (c) Reradiation interaction H_i^R, which opposes SSB. (d) $H_i^0 + H_i^S + H_i^R$, which shows slightly reduced SSB with respect to (b).

Let us first explain qualitatively the physical mechanism of the SSB shadow effect for the ith atom. We assume the right(left)-side atomic cloud corresponds to the state 1 (2). Because of the Zeeman shift, atoms in state 1 (2) absorb preferentially the cooling laser propagating in the $-z$ $(+z)$ direction. Now we consider another jth atom in state 1 or 2, which absorbs the laser by the amount $I_A^j = \sigma_L^j n_\rho I_z$, where σ_L^j is the absorption cross section of the jth atom and n_ρ is the planar atomic density in the xy plane. One then easily finds that each laser photon absorbed by the jth atom effectively results in a cooperative force on the ith atom, with the magnitude $C_S\sigma_L^j n_\rho I_z/I_s$ [refer to Eq. (3) for C_S]. That is, when the atom j is in state 1 (i.e., in the right-side cloud absorbing the photons propagating in the $-z$ axis), the force experienced by the ith atom is along the $+z$ direction, whereas it is opposite when the jth atom is in state 2. Thus the net force exerted on the ith atom, when summed over j, is given by $\sum_j C_S I_A^j/I_s = (N_1 - N_2)C_S I_A/I_s$, which is positive for $N_1 > N_2$. Therefore, the ith atom is transferred to the larger-number state on the right (i.e., state 1) [Fig. 4(b)].

Here, it is interesting to note that our symmetry breaking process occurs *spontaneously* by using an energy argument, as in the Ising spin system. Let us consider, for simplicity, two atoms oscillating on the z axis. Then it is energetically more favorable to have two atoms in the same state, rather than to have one atom in each state, because there is no shadow in the former case so that the system is stable, whereas each atom is pushed by the tiny shadow force in the latter case. In other words, the total energy of two atoms in the same state is lower than the other case. When this energy-lowering tendency (or "correlation" of the Ising system) due to shadow effect dominates, with the increase of total atomic number, the symmetry-recovering fluctuation effect due to spontaneous emission, the population symmetry becomes spontaneously broken.

A detailed formulation of the processes discussed above leads to the Hamiltonian H_i^S for the shadow effect that occurs in the Y_i axis, given by

$$H_i^S(X_i, Y_i) = \sum_{j\in 1,2}\alpha_j Y_i = \alpha(N_1 - N_2)Y_i, \quad (3)$$

where $\alpha_j = \alpha = 2C_S\sigma_L I_z/I_s\pi^2\gamma\zeta^{3/2}\eta f 2\pi R_\rho^2$ (σ_L^j is assumed independent of j), $C_S = \hbar k\Gamma/2m(1 + 4\delta^2/\Gamma^2)$, $\zeta = 2\pi h f_0^2/\gamma f$, δ is the laser detuning, and $\eta = \sqrt{4\pi\gamma f f_0^2/3A_0(\gamma^2 + 4\pi^2 f_0^2)}$. By the Monte Carlo simulation, as shown in Fig. 4(b), one can observe that the potential of the larger-number state (state 1) becomes deeper, whereas that of the smaller-number state (state 2) shallower. Thus, more atoms are transferred from state 2 to state 1, resulting in SSB of the atomic population. In fact, N_c is determined by the balance between the SSB shadow effect and the symmetry-recovering diffusive atomic motion due to spontaneous emission. Note that the latter corresponds to thermal fluctuation in the Ising model, not to magnetization fluctuation associated with the increased spin-spin correlation.

Let us now consider the symmetry-preserving collective effect of reradiation. Figure 4(c) presents the numerical results of reradiation interaction H_i^R, which reduces the SSB effect (detailed expression of H_i^R will be given elsewhere). Because of the repulsiveness of multiple photon interactions, the reradiation effect reduces the difference of potential depths of the two states, favoring equal population. This is similar to the case of a system of two connected conducting spheres of equal size where the minimum energy is obtained when the two spheres are equally charged. The analytical calculation shows that the reradiation slightly reduces the coefficient α, resulting in the increase of N_c (refer to next paragraph for the relation between N_c and α). Moreover, since the reradiation effect is proportional to the total laser intensity unlike the shadow effect which depends only on the longitudinal laser intensity, we have observed that when the transverse laser intensity is about 20 times larger than that of the z-direction laser, the reradiation effect dominates the shadow effect and thus SSB does not occur for every N_T. This is in reasonable agreement with numerical calculation and is an independent evidence that the reradiation hinders SSB.

For a simple understanding of the temporal evolution of SSB [Fig. 2(b)] and for manifestation of the relation with the Ising model, let us consider the rate equation, $d\Delta_p/dt = -W_{12}(1+\Delta_p) + W_{21}(1-\Delta_p)$, where the atomic transition rate $W_{12(21)}$ from state 1 (2) to state 2 (1) is $W_0 \exp(\mp\Delta_p N_T/N_c)$ and $N_c = [D/2\alpha\zeta\sqrt{\mu+1}f(\mu)]$. Here W_0 is the atomic transition rate without collective effects, D is the phase-space diffusion constant [10], and $f(\mu)$ is an $O(1)$ function [13]. Interestingly, the above rate equation leads to the steady-state solution given by

$$\Delta_p = \tanh(\Delta_p N_T/N_c), \qquad (4)$$

which is a representative equation of the mean-field Ising model, as plotted in Fig. 2(a). Note that Eq. (4) is associated with the infinite-dimensional Ising-model Hamiltonian, from which SSB is naturally manifested. This is experimentally justified; one can measure, from the data in Fig. 2(a), the critical exponent, β, related to the "magnetization" Δ_p. We obtained the value of 0.43 ± 0.13 and this is a signature of the mean-field universality of the second-order phase transitions that associate an exact value of 0.5 generically.

In conclusion, we demonstrated SSB of the population of cold atoms between two *moving* optical potentials in the driven system far from equilibrium. We showed the main characteristics of symmetry breaking were described by the mean-field Ising-class phase transition, that is, the Ising model in the limit of infinite dimensions. In particular, this well controlled system of driven cold atoms may not only be applied as a model system for *in situ* study of dynamic phase transition or temporal dependence of critical phenomena, but also opens up a novel optical research of cooperative phenomena in an interacting many body system. For example, improved measurements of several critical exponents of our Ising-class system are currently under progress.

This work was supported by the CRI Project of the Ministry of Science and Technology of Korea. H. R. N. was supported by Korea Research Foundation Grant (No. KRF-2005-041-C00201).

*Corresponding author.
Email address: whjhe@snu.ac.kr

[1] P. Reimann, Phys. Rep. **361**, 57 (2002), and references therein.
[2] R. D. Astumian, Science **276**, 917 (1997).
[3] M. M. Millonas and D. R. Chialvo, Phys. Rev. E **53**, 2239 (1996); M. Arrayas *et al.*, Phys. Rev. Lett. **84**, 5470 (2000); R. Gommers *et al.*, Phys. Rev. Lett. **94**, 143001 (2005).
[4] J. C. Maxwell, *Theory of Heat* (Greenwood, Westport, 1970), 3rd ed.
[5] J. Eggers, Phys. Rev. Lett. **83**, 5322 (1999); T. Shinbrot and F. J. Muzzio, Nature (London) **410**, 251 (2001).
[6] K. Kim *et al.*, Phys. Rev. A **68**, 031403(R) (2003).
[7] J. Dalibard, Opt. Commun. **68**, 203 (1988).
[8] D. E. Sesko, T. G. Walker, and C. E. Wieman, J. Opt. Soc. Am. **B8**, 946 (1991).
[9] L. P. kadanoff, *Statistical Physics: Statics, Dynamics and Renormalization* (World Scientific, Singapore, 2000).
[10] K. Kim *et al.*, Phys. Rev. A **72**, 053402 (2005).
[11] V. S. Bagnato *et al.*, Phys. Rev. A **48**, 3771 (1993); D. Felinto *et al.*, Phys. Rev. A **60**, 2591 (1999).
[12] D. Wilkowski *et al.*, Phys. Rev. Lett. **85**, 1839 (2000).
[13] M. I. Dykman *et al.*, Phys. Rev. E **57**, 5202 (1998).